Published OnlineFirst January 12, 2010; DOI: 10.1158/0008-5472.CAN-09-2189

Clinical Studies

Cancer Research

Reversing *HOXA9* Oncogene Activation by PI3K Inhibition: Epigenetic Mechanism and Prognostic Significance in Human Glioblastoma

Bruno M. Costa[1,2], Justin S. Smith[1], Ying Chen[1], Justin Chen[1], Heidi S. Phillips[3], Kenneth D. Aldape[4], Giuseppe Zardo[1,5], Janice Nigro[6], C. David James[1], Jane Fridlyand[1], Rui M. Reis[2], and Joseph F. Costello[1]

Abstract

HOXA genes encode critical transcriptional regulators of embryonic development that have been implicated in cancer. In this study, we documented functional relevance and mechanism of activation of *HOXA9* in glioblastoma (GBM), the most common malignant brain tumor. Expression of *HOXA* genes was investigated using reverse transcription–PCR in primary gliomas and glioblastoma cell lines and was validated in two sets of expression array data. In a subset of GBM, *HOXA* genes are aberrantly activated within confined chromosomal domains. Transcriptional activation of the *HOXA* cluster was reversible by a phosphoinostide 3-kinase (PI3K) inhibitor through an epigenetic mechanism involving histone H3K27 trimethylation. Functional studies of HOXA9 showed its capacity to decrease apoptosis and increase cellular proliferation along with tumor necrosis factor–related apoptosis-including ligand resistance. Notably, aberrant expression of *HOXA9* was independently predictive of shorter overall and progression-free survival in two GBM patient sets and improved survival prediction by *MGMT* promoter methylation. Thus, *HOXA9* activation is a novel, independent, and negative prognostic marker in GBM that is reversible through a PI3K-associated epigenetic mechanism. Our findings suggest a transcriptional pathway through which PI3K activates oncogenic *HOXA* expression with implications for mTOR or PI3K targeted therapies. *Cancer Res; 70(2); 453–62. ©2010 AACR.*

Introduction

Glioblastoma (GBM) is the most common and malignant primary brain tumor in adults. With rare exception, the infiltrative nature of GBM precludes surgical cure and adjuvant therapies have achieved only modest benefit, with median survival remaining ~12 months (1). Specific molecular characteristics of GBM can be used to define prognostic subgroups (2–4). *MGMT* promoter methylation (5, 6) is an independent favorable prognostic factor for GBM patients (3), but this marker does not fully account for the variability in survival (3), and additional markers are needed to be used for the prognosis of individual patients.

Homeobox genes encode transcription factors important for antero-posterior patterning during embryogenesis. In humans, there are 39 Class I homeobox (*HOX*) genes found in four genomic clusters (*HOXA* at 7p15.3, *HOXB* at 17q21.3, *HOXC* at 12q13.3, and *HOXD* at 2q31). Their spatial and temporal colinear expression pattern is critical for body patterning during development (7, 8), and *HOX* genes also have critical postdevelopmental regulatory functions (9–12). Aberrant *HOX* gene expression initiates leukemias (13, 14), contributes to multiple types of solid tumors (15, 16), and has been detected in malignant astrocytomas (17). Furthermore, *HOXA9* and *MEIS1* may be part of a switch that regulates progenitor abundance by suppressing differentiation and maintaining self-renewal during myelopoiesis (18). Thus, among the 39 *HOX* genes, *HOXA9* is of particular importance in leukemia and potentially other cancers.

In the present study, we identify a subgroup of GBMs with chromosomal domains of aberrant *HOX* gene activation, show a mechanism by which this domain of activation is reversible, define an association between *HOXA9* expression and poor clinical outcome, and provide functional data on the effects of HOXA9 in cell proliferation and apoptosis.

Authors' Affiliations: [1]The Brain Tumor Research Center, Department of Neurological Surgery, University of California-San Francisco, San Francisco, California; [2]Life and Health Sciences Research Institute (ICVS), School of Health Sciences, University of Minho, Braga, Portugal; [3]Department of Tumor Biology and Angiogenesis, Genentech, Inc., South San Francisco, California; [4]Department of Pathology, M.D. Anderson Cancer Center, Houston, Texas; [5]Department of Cellular Biotechnologies and Hematology, University of Rome-La Sapienza, Rome, Italy; and [6]University of Bergen-Institute of Biomedicine, Bergen, Norway

Note: Supplementary data for this article are available at Cancer Research Online (http://cancerres.aacrjournals.org/).

B.M. Costa and J.S. Smith contributed equally to this work.

Corresponding Author: Joseph F. Costello, University of California San Francisco, Helen Diller Family Cancer Research Building, 1450 3rd Street, Room 285, San Francisco, CA 94158-9001. Phone: 415-514-1183; Fax: 415-514-9001; E-mail: jcostello@cc.ucsf.edu.

doi: 10.1158/0008-5472.CAN-09-2189

Published OnlineFirst January 12, 2010; DOI: 10.1158/0008-5472.CAN-09-2189

Materials and Methods

Human tissues and glioma cell models. Human tissue samples were obtained from the Neurosurgery Tissue Banks at University of California, San Francisco (UCSF) and M.D. Anderson Cancer Center (MDA) and would have been otherwise discarded. Tumor samples were examined by a neuropathologist to ensure that >90% of the tissue represented tumor and classified according to current WHO guidelines (19). All samples were collected with informed consent, and investigations using human tissues and clinical data were approved by the institutional review boards of UCSF and MDA. Initial exploratory survival analysis was performed on a set of nine GBMs from UCSF. Validation of a trend between *HOXA9* expression and poor survival was performed using two sets of expression array data (Affymetrix U133 arrays or Affymetrix U95Av2 arrays), one set consisting of 37 GBM samples from UCSF (20) and a second set composed of 63 GBMs from MDA (ref. 21; Gene Expression Omnibus accession number GSE4271). Combined assessment of *HOXA9* expression and *MGMT* promoter methylation was performed in 35 of the 37 GBMs from UCSF. Details of the tumor types and nontumor samples are included in the online Supplementary Materials and Methods. The nine GBM cell lines (A172, LN18, LN215, LN229, LN235, LN319, U87-MG, U178, and U373) and immortalized human astrocytes (hTERT/E6/E7) were maintained in DMEM with 10% fetal bovine serum, the neurospheres were maintained in neurobasal medium supplemented with basic fibroblast growth factor and epidermal growth factor (21), and the orthotopic xenografed GBMs were derived as previously described (22–24).

In vitro *analyses.* RNA isolation, cDNA synthesis, reverse transcription–PCR (RT-PCR), quantitative real-time PCR (qPCR), and chromatin immunoprecipitation (ChIP) analyses were performed by standard techniques in cell lines (Supplementary Materials and Methods). DNA isolation, bisulfite treatment, and analyses of *MGMT* promoter methylation in primary tumor tissues from UCSF were performed as described previously (3, 25) and are detailed in Supplementary Materials and Methods. A172 cells and neurospheres were treated with a phosphoinositide 3-kinase (PI3K) inhibitor (LY294002) and rapamycin to investigate the mechanism regulating *HOXA* gene expression in GBM. Overexpression of *HOXA9* by retroviral infection and siRNA-mediated silencing of *HOXA9* were used to investigate the functional relevance of *HOXA9* expression, which was assessed by cell proliferation and apoptosis analyses (Supplementary Materials and Methods).

Statistical analyses. The Kaplan-Meier method was used to estimate overall survival (OS) and progression-free survival (PFS), where OS was measured from the time of surgical resection to death or the last date when the patient was known to be alive, and PFS was defined as the time from surgical resection to the time of shown tumor growth on follow-up imaging or death, if death occurred before documented progression. Multivariate survival analyses by Cox proportional hazard models (backward selection) were performed to adjust for the effects of patient age and Karnofsky performance status (KPS). A P value of <0.05 was considered significant.

The two-sided Student's t test was used to assess statistical differences in qPCR data and *in vitro* cell death and apoptosis experiments. A repeated measures ANOVA was used to assess differences in the cell proliferation curves.

To identify samples that express a given gene and assign the confidence to each sample, we used model-based clustering to identify the mixture components. Analysis of gene expression microarray data, generation of heat maps for the *HOX* clusters, and investigation of correlations between expression of *HOXA9* and other transcripts are detailed in Supplementary Materials and Methods.

Results

HOXA *genes are predominantly activated in high-grade astrocytoma.* Initially, we assessed *HOXA* gene expression in normal brain tissue, primary diffuse glioma tissue, and GBM-derived cell lines using RT-PCR. Most *HOXA* genes were not expressed in fetal and adult nontumoral brain tissues (Fig. 1*A*). Similarly, of eight primary grade 2 and grade 3 gliomas, *HOXA* gene expression was evident in only two cases (Fig. 1*A*). In contrast, all primary GBMs and cell lines showed expression of multiple *HOXA* genes (Fig. 1*A*). Supplementary Fig. S1*A* shows representative RT-PCR analyses of *HOXA* gene expression in human astrocytoma samples, exemplifying tumors that were positive or negative for expression of specific *HOXA* genes. Collectively, these data suggest that aberrant *HOXA* gene expression is a common feature of the most malignant gliomas, GBM, and infrequent in lower-grade gliomas.

HOXA9 was the only *HOXA* gene whose expression showed a trend to associate with shorter survival of these nine GBM patients (median survival of 9 versus 53 weeks, $P = 0.06$). Supplementary Fig. S1 (*B* and *C*) suggests *HOXA9* expression in GBMs is not simply a reflection of the expression pattern of the tumor cell(s) of origin nor a consequence of therapeutic agents but rather represents an aberrant gene activation event associated with tumor progression.

A confined chromosomal domain of transcriptional activation encompasses* HOXA *expression in GBM. We next analyzed expression of *HOXA* genes in two independent validation sets of expression array data, one set of 37 GBMs from UCSF (20) and a second set of 63 GBMs from MDA (21). To investigate whether aberrant *HOXA* activation was an isolated event, or part of a larger chromosomal mechanism, we created heat maps for the *HOXA* cluster and surrounding genes within 1 Mb in each direction (Fig. 1*B*). In both sets, the *HOXA* cluster showed a distinct chromosomal domain of activation such that many of the *HOXA* genes were concurrently activated, whereas genes outside of the domain were mostly silent (Fig. 1*B*). Similar domains of transcriptional activation were also present in the *HOXB, HOXC*, and *HOXD* clusters (Supplementary Fig. S2 and S3), suggesting a common, coordinated activation of these domains.

Heat map analyses reflecting the expression pattern across all four *HOX* clusters in UCSF and MDA tumor sets analyzed

Published OnlineFirst January 12, 2010; DOI: 10.1158/0008-5472.CAN-09-2189

by expression arrays (Supplementary Fig. S4) revealed that (*a*) a subset of GBMs shows widespread activation of *HOX* genes, (*b*) the pattern of *HOX* activation is aberrant and does not resemble the coordinated colinear expression observed during normal embryonic development, (*c*) *HOXA9* substantially contributes to the clustering into two sample groups in both data sets. To quantify which of the *HOX* genes account for the clustering, the fold change between the two groups for each gene was computed using the median value of the genes in each group (Supplementary Table S1). The *HOX* genes with statistically significant different expression between the two heat map cluster groups in both the UCSF and MDA tumors are *HOXA1-A5, HOXA7, HOXA9, HOXA10, HOXB7*, and *HOXC6*.

We used the ONCOMINE database to investigate additional GBM expression array data sets for activation of the *HOXA* domain (26). A subset of GBM patients showed a similar profile of activation of *HOXA* genes in a study by Sun and colleagues (27). Expression of most *HOXA* genes, with the exception of *HOXA6* and *HOXA13*, showed a high positive correlation with *HOXA9* expression (Supplementary Table S2). *HOXA11*, which did not show a statistically significant positive correlation with *HOXA9* expression in our tumor sets, also showed a substantially lower correlation coefficient in the samples from Sun and colleagues (27). Because *HOXA6* and *HOXA13* do not correlate with *HOXA9* expression in all three tested tumor sets, a mechanism of chromosomal amplification encompassing the entire *HOXA* locus may not adequately explain the presence of such transcriptionally active domains. Furthermore, we confirmed in the UCSF set that aberrant *HOXA* gene activation may be enhanced by, but is not reliant on, increased chromosome 7p15.3 copy number ($P = 0.5$, data not shown).

Inhibition of the PI3K pathway reverses aberrant transcriptional activation of the* HOXA *cluster. In HeLa cells, the PI3K signaling pathway can regulate EZH2 activity (28), a key component of the polycomb repressor complex 2 that promotes gene silencing by trimethylation of histone H3 lysine 27 (H3K27-3met) on target genes. AKT-mediated phosphorylation of EZH2 inhibits its histone methyltransferase activity, resulting in gene reactivation. Given that *HOXA* genes are known targets of EZH2-mediated methylation in some normal tissues (29) and that *PTEN*, a regulator of PI3K activity, is frequently inactivated in GBM (30, 31), we hypothesized that alterations in the PI3K pathway may be upstream effectors of aberrant *HOXA* gene expression in GBM. We first investigated a potential relationship between PI3K signaling and *HOXA9* expression in A172 cells, a GBM cell line with *PTEN* homozygous deletion (32) and *HOXA9* activation. Consistent with the PI3K pathway having a regulatory function on *HOXA9* expression, *HOXA9* transcript levels were significantly reduced in A172 cells after treatment with the PI3K inhibitor LY294002 (Supplementary Fig. S5*A*). This regulatory mechanism was reversible as *HOXA9* was restored to pretreatment levels 32 hours after A172 cells were placed in fresh medium lacking LY294002 (Supplementary Fig. S5*A*). The levels of HOXA9 protein were also decreased in LY294002-treated cells at 24 h (Supplementary Fig. S5*B*). Considering the concomitant activation of several *HOXA* genes within domains of activation in primary GBMs, we hypothesized that *HOXA* genes in GBM are activated by a shared mechanism of transcriptional regulation. To address this question, the entire *HOXA* cluster was tested for suppression by LY294002 treatment of A172 cells. Expression of most *HOXA* genes was suppressed (range, 39–74%) after treatment with LY294002, except for *HOXA6* and *HOXA13* (Fig. 2*A*); these two *HOXA* genes also did not correlate with *HOXA9* expression in our primary tumor sets (Supplementary Table S1) or in the cohort studied by Sun and colleagues (27). These data suggest that *HOXA9* expression is reversibly regulatable by the PI3K pathway in glioma cells and further suggest that this regulation extends throughout most of the 100+ kb chromosomal domain containing the *HOXA* cluster.

To further support our data implicating the PI3K pathway as a critical regulatory mechanism of *HOXA* gene expression, we next searched the Connectivity Map data set for drugs that induce gene expression signatures involving *HOXA9*-associated genes (33). This analysis revealed common PI3K inhibitors, including LY294002 and Wortmannin, as top hits significantly associated with the *HOXA9*-derived gene expression signature (Supplementary Table S3 and Supplementary Results: Connectivity Map analyses reveal the PI3K pathway as a key regulator of *HOXA* genes expression). Additionally, in primary GBM xenografts derived from 18 patients, aberrant activation of *HOXA9* was significantly associated with *PTEN* gene inactivation [*PTEN* mutations and homozygous deletion were previously examined by sequence analysis and multiplex PCR analysis, respectively (22, 24)], further supporting the relevance of PI3K signaling for the regulation of *HOXA* expression (Supplementary Table S4 and Supplementary Results: aberrant expression of *HOXA9* is associated with *PTEN* gene inactivation in primary GBM xenografts).

Therapeutic agents that inhibit mTOR, a downstream mediator of the PI3K pathway, are currently in clinical trials for GBM. To determine whether mTOR is a critical regulator of *HOXA* gene expression, A172 cells were treated with rapamycin, an inhibitor of mTOR activity, and the expression levels of the *HOXA* genes were assessed by RT-PCR. Rapamycin treatment resulted in a more modest inhibition of *HOXA* transcripts levels (Fig. 2*B*), suggesting that the mechanism by which the PI3K pathway regulates *HOXA* genes expression is primarily independent of mTOR. HOXA9 protein levels were also unaffected by rapamycin treatment as indicated by immunoblotting analysis (Supplementary Fig. S5*C*).

To determine whether the PI3K-mediated regulation of *HOXA* genes is also observed in other GBM cell lines, we tested how LY294002 treatment affected *HOXA9* levels by qPCR in two sublines of a primary GBM grown in neurosphere conditions, both of which presented detectable levels of endogenous *HOXA9*. Similarly to the observations in A172 cells, the inhibition of PI3K in these neurospheres also repressed *HOXA9* mRNA levels (Supplementary Fig. S5*D*), whereas the relationship between rapamycin and *HOXA9* expression in the very small number of neurosphere lines is not as consistent (Supplementary Fig. S5*E*).

Published OnlineFirst January 12, 2010; DOI: 10.1158/0008-5472.CAN-09-2189

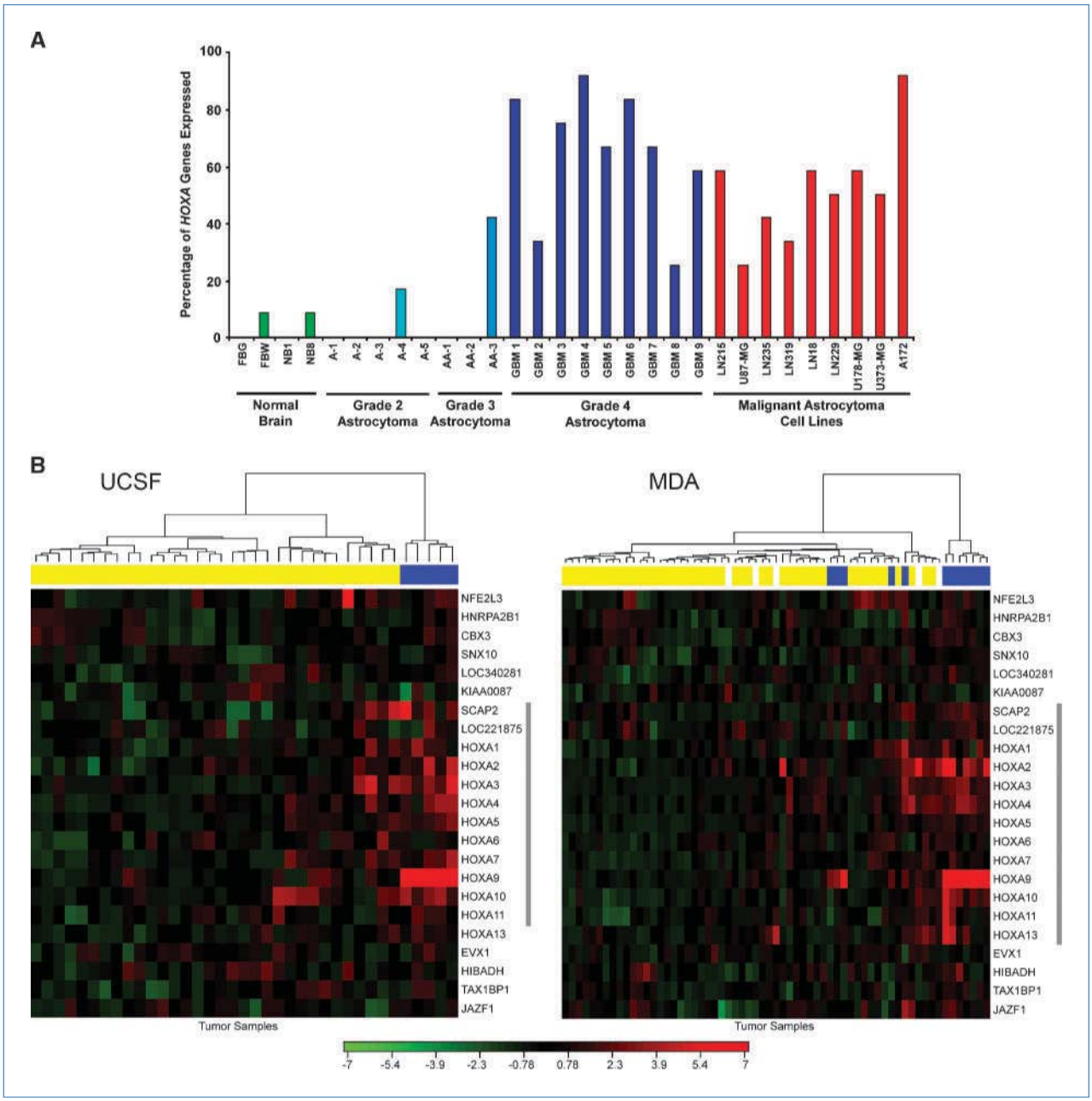

Figure 1. *HOXA* genes are activated predominantly in high-grade astrocytoma. *A,* percentage of *HOXA* genes with detectable levels of expression by RT-PCR in normal brain tissue, in primary tumor tissue (astrocytoma WHO grades 2–4), and in established malignant GBM cell lines. Fetal brain gray (*FBG*) matter and fetal brain white (*FBW*) matter are nonneoplastic tissues from human fetal brain. NB1 and NB8 are nonneoplastic adult brain specimens. *A,* astrocytoma (WHO grade 2); *AA,* anaplastic astrocytoma (WHO grade 3); *GBM,* glioblastoma (WHO grade 4). *B,* gene expression heat maps centered on the *HOXA* cluster and extending 1 Mb in each direction. Both UCSF (*left*, 37 tumors) and MDA (*right*, 63 tumors) sets show *HOXA* gene domains of transcriptional activation, such that genes contained in the boundaries flanking the activated domains are relatively silent. One exception is *SCAP2*, located ~200 kb outside of the *HOXA* cluster. The gray vertical bars indicate the approximate boundaries of the domain of activation. The colored bars across the top of the heat maps indicate which tumors express *HOXA9* [*blue,* high expression; *yellow,* low or no expression; *white,* samples for which the expression status could not be assigned with high (>95%) confidence]. Red and green colors on the heat map reflect high and little/no expression of each gene, respectively.

PI3K-mediated regulation of* HOXA9 *gene expression occurs through reversible epigenetic histone modifications. To elucidate the downstream effectors of PI3K-mediated regulation of *HOXA* gene expression and considering that AKT mediates EZH2 histone methyltransferase activity in HeLa cells, we assessed whether the regulatory role of the PI3K pathway on *HOXA9* expression could be linked to histone modifications. ChIP analysis was performed on A172 cells

Published OnlineFirst January 12, 2010; DOI: 10.1158/0008-5472.CAN-09-2189

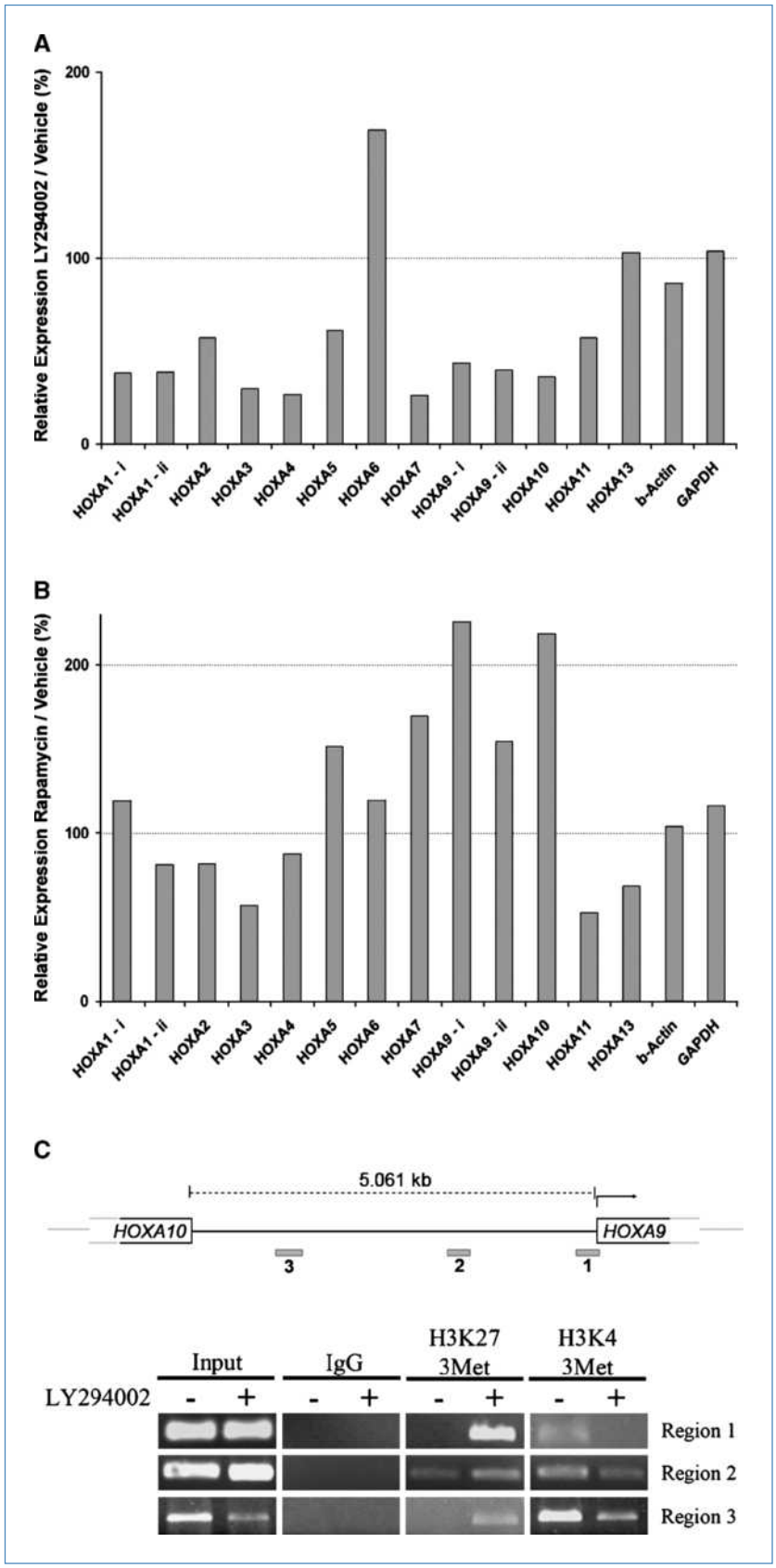

Figure 2. The PI3K pathway regulates *HOXA* cluster gene transcription in GBM through reversible epigenetic histone modifications, independently of mTOR. *A,* expression levels of genes in the *HOXA* cluster by RT-PCR after treatment of A172 cells with the PI3K inhibitor LY294002. *β-Actin* and *glyceraldehyde-3-phosphate dehydrogenase* (*GAPDH*) were used as control genes. Values are ratios of expression levels in treated/untreated A172 cells for each *HOXA* gene. Expression of most *HOXA* genes, except for *HOXA6* and *HOXA13*, decreased after PI3K inhibition. *HOXA1* and *HOXA9* expression was assessed for each of two alternative splicing forms (*i* and *ii*). The results are representative of three independent experiments. *B,* expression levels of *HOXA* genes after treatment with rapamycin, a specific mTOR inhibitor. Data are presented similarly to *A*. The results are representative of three independent experiments. *C,* ChIP analysis of the *HOXA9* 5′ region after LY294002-mediated inhibition of PI3K. *Top,* diagram indicating the locations of the primer sets used for ChIP analysis. *Bottom,* PCR products for the three regions after ChIP analysis in A172 cells treated with LY294002 (+) or vehicle (–). The input products reflect PCR on DNA not selected by immunoprecipitation. The IgG reaction serves as a negative control. The results are representative of three independent experiments.

Published OnlineFirst January 12, 2010; DOI: 10.1158/0008-5472.CAN-09-2189

that were either untreated or treated with LY294002 for 24 hours. A172 cells treated with LY294002 showed reduced expression of *HOXA9*, as well as reduced H3K4 trimethylation (a mark of active chromatin) and concomitant increased H3K27 trimethylation (a mark of repressive chromatin) in three different regions near the *HOXA9* promoter (Fig. 2*C*). When LY294002-treated cells were incubated for an additional 48 hours in fresh media without drug, *HOXA9* expression, H3K27 trimethylation, and H3K4 trimethylation returned to pretreatment levels (data not shown). Collectively, these data indicate that the regulatory role of the PI3K pathway on *HOXA9* expression is linked to epigenetic histone modifications that seem to be fully and expediently reversible in GBM cells.

HOXA9 ***increases cell proliferation and inhibits apoptosis.*** To test the functional consequences of *HOXA9* overexpression *in vitro*, a GBM cell line (U87-MG) and immortalized human astrocytes (hTERT/E6/E7) stably overexpressing *HOXA9* were established by retroviral infection and compared with their counterparts infected with control vector, which do not overexpress *HOXA9* (Fig. 3*A*). The use of these two GBM models allowed us to test the effect of *HOXA9* overexpression in tumoral (U87-MG) and immortalized but nontumoral (hTERT/E6/E7) backgrounds. Expression of exogenous *HOXA9* was associated with a modest but consistent increase in proliferation of hTERT/E6/E7 cells (Fig. 3*B*; $P < 0.001$) and a decrease in their spontaneous apoptosis (Fig. 3*C*; $P = 0.032$) compared with the parental cells. U87-MG cells stably expressing exogenous *HOXA9* consistently showed a modest increase in proliferation, but only when the cells became more confluent (Fig. 3*B*; $P < 0.001$). *HOXA9* expression in U87-MG cells also decreased tumor necrosis factor–related apoptosis-inducing ligand (TRAIL)–induced apoptosis (Fig. 3*C*; $P = 0.009$). These data suggest that HOXA9 serves an antiapoptotic role in immortalized human astrocytes and GBM cells, which may affect cell number/proliferation. Conversely, the inhibition of endogenous *HOXA9* expression in A172 cells with siRNA (Fig. 3*D*) resulted in increased spontaneous apoptosis

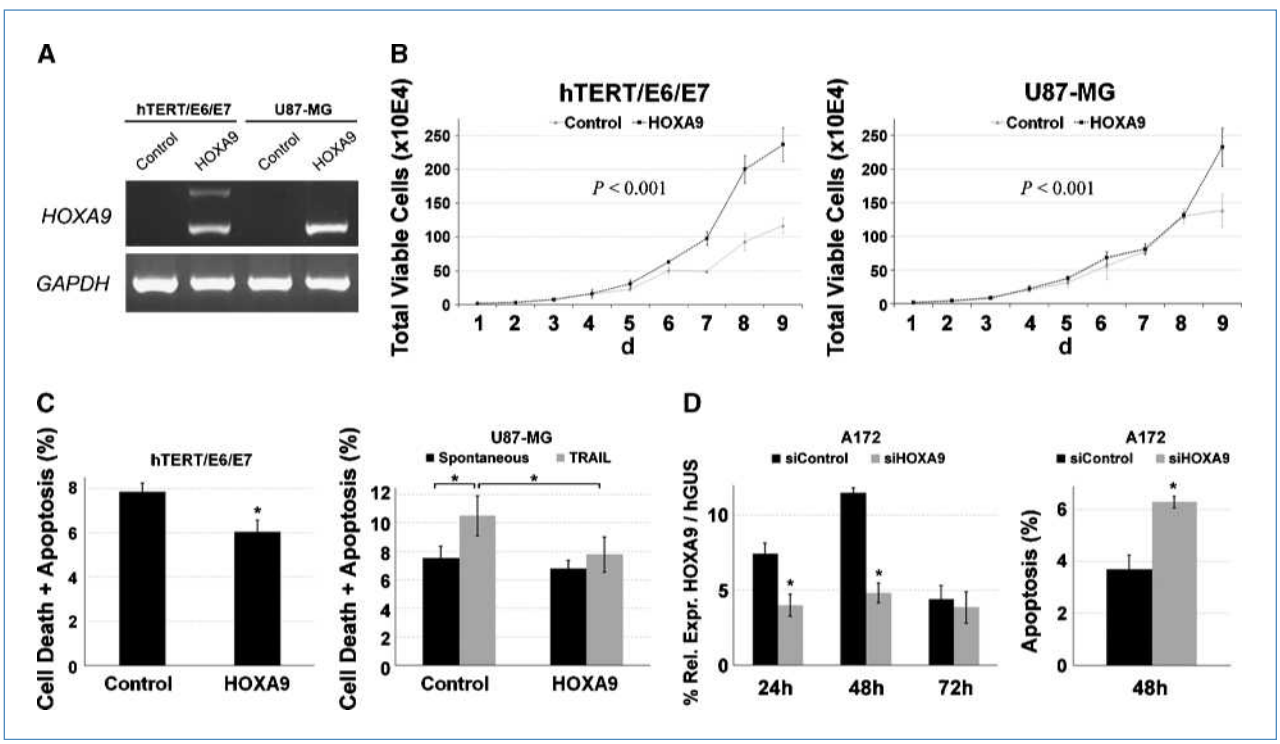

Figure 3. Expression of *HOXA9* influences cell proliferation and apoptosis. *A,* immortalized human astrocytes (hTERT/E6/E7) and a GBM-derived cell line (U87-MG) were retrovirally infected with a MSCV-HOXA9 construct or control vector and tested for *HOXA9* expression by RT-PCR. *Glyceraldehyde-3-phosphate dehydrogenase* (*GAPDH*) was used for equal loading control. Successful expression of exogenous *HOXA9* was detected for both cell types. The two PCR bands for *HOXA9* derive from amplification of specific alternative splicing isoforms. *B,* proliferation curves of hTERT/E6/E7 and U87-MG cells after retroviral infections. Results are representative of three independent experiments, and each time point was counted in duplicate (data points represent mean ± SD). Repeated measures ANOVA showed statistically significant differences between control cells and cells overexpressing *HOXA9* (hTERT/E6/E7/Control versus hTERT/E6/E7/HOXA9, $F_{(1,18)} = 92.7$, $P < 0.001$; U87-MG/Control versus U87-MG/HOXA9, $F_{(1,18)} = 19.7$, $P < 0.001$). *C,* apoptosis analysis by Annexin V–FITC and propidium iodide staining followed by flow cytometry. Results are representative of three independent experiments (averages ± SDs), each showing a similar effect relative to controls. *, $P < 0.05$, two-sided Student's *t* test ($P = 0.032$ for hTERT/E6/E7/Control versus hTERT/E6/E7/HOXA9; $P = 0.036$ for spontaneous U87-MG/Control versus TRAIL-treated U87-MG/Control; $P = 0.009$ for TRAIL-treated U87-MG/Control versus TRAIL-treated U87-MG/HOXA9). *D, left,* qPCR analysis of *HOXA9* expression levels after treatment with siHOXA9 or siControl for various time points. Expression levels were normalized to *hGUS*. *, $P < 0.05$, two-sided Student's *t* test ($P = 0.004$ for 24 h; $P = 0.001$ for 48 h). *Right,* apoptosis analysis by Annexin V–FITC and propidium iodide staining followed by flow cytometry 48 h after siRNA treatments. The results are representative of three independent experiments (averages ± SDs), each showing a similar effect relative to controls. *, $P = 0.026$, two-sided Student's *t* test.

Published OnlineFirst January 12, 2010; DOI: 10.1158/0008-5472.CAN-09-2189

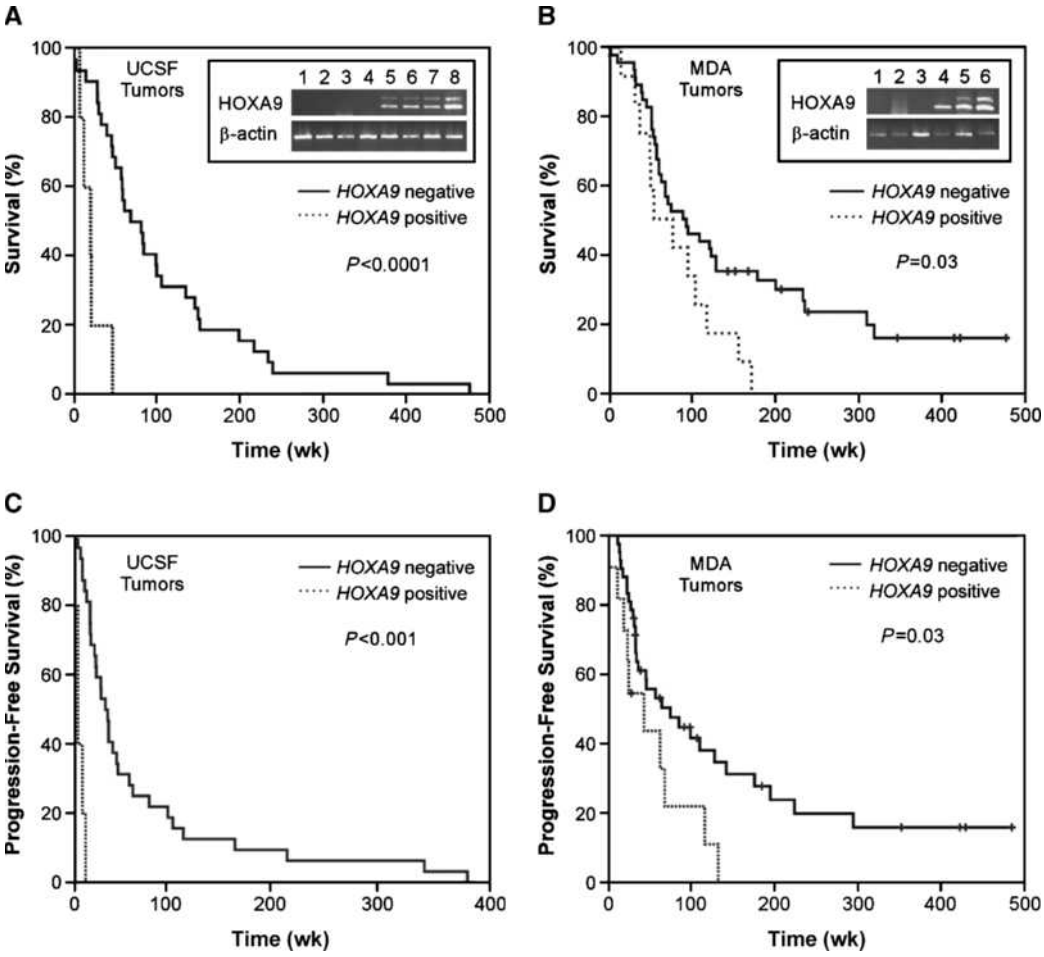

Figure 4. *HOXA9* expression is associated with OS and PFS of GBM patients. *A* and *B,* Kaplan-Meier (*KM*) OS curves for GBM patients from UCSF (*A*) and MDA (*B*), whose tumors do express (*dotted line*) and do not express (*solid line*) *HOXA9*, as assessed by expression array analysis. The inset provides RT-PCR confirmation of *HOXA9* expression status in tumors classified as nonexpressers (lanes 1–4 in the UCSF set; lanes 1–3 in the MDA set) and tumors classified as expressers (lanes 5–8 in the UCSF set; lanes 4–6 in the MDA set), based on expression array analysis in each set. Vertical tic marks indicate censored data time points. *C* and *D,* Kaplan-Meier PFS curves for the same GBM sets. Vertical tic marks indicate censored data time points.

(Fig. 3*D*), further supporting an antiapoptotic role of HOXA9 in GBM cells.

HOXA9 ***expression is associated with shorter OS and PFS in GBM patients.*** Based on the association of *HOXA9* with poor prognosis in the initial test set of nine GBM patients, we then performed survival analysis using the UCSF and MDA sets of expression array data (21). To validate the expression array data, RT-PCR for *HOXA9* was performed on the subsets of cases with the highest and lowest *HOXA9* expression array values, and the results were concordant (Fig. 4*A* and *B, insets*). In the UCSF cohort, GBM patients whose tumors expressed *HOXA9* (5 of 37, 14%) had a significantly shorter OS [median, 22 weeks; 95% confidence interval (CI), 5–38 weeks] compared with those whose tumors lacked expression of *HOXA9* (median, 68 weeks; CI, 36–100 weeks; $P < 0.0001$; Fig. 4*A*). Similarly, in the MDA set, patients whose tumors expressed *HOXA9* (14 of 63, 22%) had a shorter median OS (56 weeks; CI, 10–102 weeks) than those whose tumors lacked *HOXA9* expression (median OS, 91 weeks; CI, 46–136 weeks; $P = 0.03$; Fig. 4*B*). Patients whose tumors expressed *HOXA9* also had significantly shorter PFS. Median PFS was 4 weeks (CI = 4–5 weeks) and 30 weeks (CI = 22–38 weeks) in the UCSF set and 46 weeks (CI = 17–76 weeks) and 77 weeks (CI = 22–132 weeks) in the MDA set for patients whose tumors did and did not express *HOXA9*, respectively ($P < 0.0001$, Fig. 4*C*, UCSF set; $P = 0.03$, Fig. 4*D*, MDA set). These associations remained statistically significant after adjusting for the effects of patient age and KPS in the UCSF set ($P = 0.006$ for OS, $P = 0.01$ for PFS). KPS data were not available for the MDA cohort.

HOXA9 ***expression status improves*** **MGMT**-***based survival prediction in GBM patients.*** *MGMT* promoter methylation in tumor tissue is currently the most powerful molecular prognostic indicator of favorable prognosis in

Published OnlineFirst January 12, 2010; DOI: 10.1158/0008-5472.CAN-09-2189

GBM (3). However, a significant subset of patients whose tumors show *MGMT* promoter methylation do not experience survival benefit. To contrast the prognostic significance of *HOXA9* expression with this biomarker standard, we performed methylation-specific PCR analysis on DNA available from 34 of the 37 UCSF GBMs previously analyzed by expression array (Fig. 1*B*) and from the original nine GBMs analyzed by RT-PCR (Fig. 1*A*). No DNA was available from the MDA set to perform methylation-specific PCR. *MGMT* promoter methylation was identified in 24 of the 43 cases (56%; Supplementary Fig. S7); as expected (3), these patients showed trends toward longer OS ($P = 0.1$; Fig. 5*A*) and PFS ($P = 0.06$; Supplementary Fig. S6*A*) compared with those whose tumors lacked *MGMT* methylation. *HOXA9* and *MGMT* in combination showed statistically significant associations with OS and PFS. Patients whose tumors showed *HOXA9* expression and/or lack of *MGMT* promoter methylation had significantly shorter OS (median, 31 weeks; CI, = 3–60 weeks) and PFS (median, 13 weeks; CI, 5–20 weeks) compared with patients whose tumors lacked *HOXA9* expression and had *MGMT* promoter methylation (median, 82 weeks; CI, 41–123 weeks for OS; $P = 0.002$; Fig. 5*B*; median, 33 weeks; CI, 22–44 weeks for PFS; $P = 0.001$; Supplementary Fig. S6*B*). These associations remained statistically significant after adjusting for the effects of patient age and KPS ($P = 0.02$ for OS, $P = 0.03$ for PFS). Expression of *HOXA9* was identified in five (21%) of the tumors with a methylated *MGMT* promoter and, among these patients, was associated with a significantly shorter OS (median survival of 9 versus 98 weeks, $P < 0.0001$; Fig. 5*C*) and shorter PFS (median PFS of 4 versus 33 weeks, $P < 0.0001$; Supplementary Fig. S6*C*).

Discussion

Multiple *HOX* genes have been shown to be overexpressed in GBM cell lines and primary astrocytomas (17), suggesting a role for these genes in gliomagenesis. However, the mechanisms underlying *HOX* activation, in addition to their functional relevance in GBM cells, have not been explored. Our results define PI3K-regulatable chromosomal domains of transcriptional activation as a means of aberrant gene expression in cancer. This adds to a growing perspective on chromosomal domains of epigenetic silencing in normal and malignant cells (34–36). The domains of *HOXA* transcriptional activation we discovered have notable features: (*a*) they involve an important set of genes, which have critical roles in embryonic development, normal adult tissue function, and oncogenesis; (*b*) they are mediated through reversible epigenetic histone modifications that are regulatable through the PI3K pathway, a pathway known to be frequently altered in many cancers (37); and (*c*) they include aberrant expression of the oncogenic *HOXA9* (13, 38), associated with histologic malignant progression, shorter time to tumor progression and shorter OS in GBM patients. Our functional data provide further support for an oncogenic role of HOXA9 in GBM. Furthermore, a recent study suggested *HOX* genes may be part of a glioma stem cell signature with prognostic significance in GBM patients treated with concomitant chemoradiotherapy (16). Our data identify PI3K pathway dysfunction as a potential driver of this signature and suggest the exciting possibility that PI3K inhibitors may allow therapeutic reversal of the core element of this cancer stem cell signature.

We implicate the PI3K pathway in the generation of aberrant *HOXA* domains of activation in GBM. Activation of the PI3K pathway in glioma is significantly associated with increasing tumor grade, decreased apoptosis, and adverse clinical outcome (37). In addition, PTEN, a central regulator of the PI3K pathway, is frequently altered in GBM and, when altered in lower-grade gliomas, portends a dismal prognosis (1). Although multiple downstream mediators of the PI3K pathway have been described and much focus is placed on translational effects of PI3K pathway dysregulation, we propose that the pathway arm involving EZH2, a central member of the polycomb repressive complexes with intrinsic

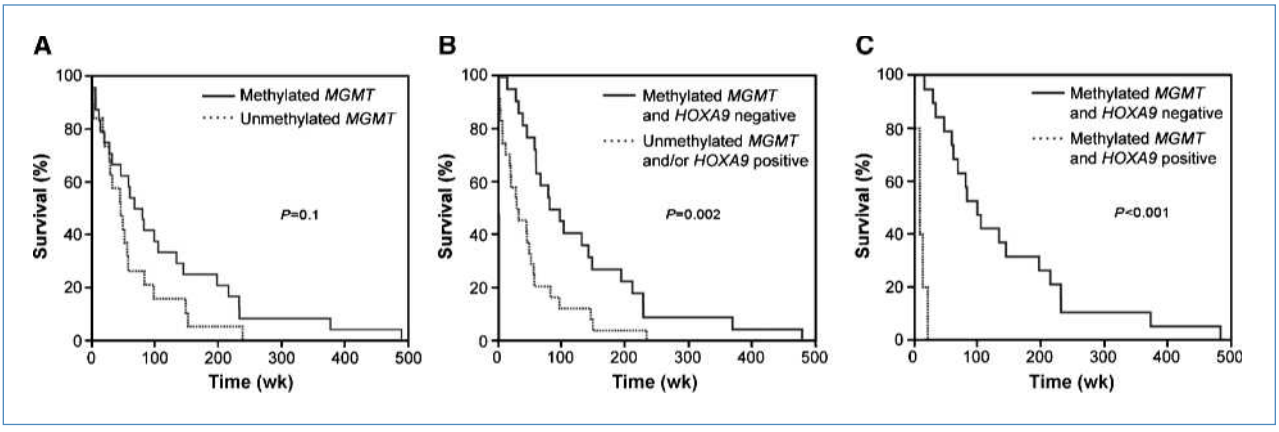

Figure 5. *HOXA9* expression improves *MGMT*-based survival prediction of GBM patients. *A,* Kaplan-Meier OS curve for 43 GBM patients from UCSF (including cases used for expression array analysis and those used for initial assessment of *HOXA* expression) whose tumors showed (*solid line*) or lacked (*dotted line*) *MGMT* promoter methylation. *B,* Kaplan-Meier OS curve for the same set as in *A*, based on *HOXA9* expression and *MGMT* promoter methylation status. *C,* Kaplan-Meier OS curve for the 24 patients whose tumors showed *MGMT* promoter methylation, stratified based on whether the tumors expressed *HOXA9*.

Published OnlineFirst January 12, 2010; DOI: 10.1158/0008-5472.CAN-09-2189

histone methyltransferase activity (39), mediates the PI3K-dependent transcriptional regulation of *HOXA9* and potentially the whole *HOXA* cluster and many other genes. Akt-mediated phosphorylation of EZH2 suppresses trimethylation of lysine 27 in histone H3 (H3K27) by interfering with the ability of the EZH2 complex to interact with histone H3, leading to derepression of silenced genes (28). EZH2 can increase cancer cell proliferation when overexpressed (40), is associated with metastasis in prostate cancer (41), and is expressed at significantly higher levels in GBM tissue versus noncancerous brain tissue (26, 27) and low-grade gliomas (26, 42). Furthermore, *EZH2* itself was among the genes that showed coexpression with *HOXA9* based on expression array data from both UCSF and MDA tumor sets. However, the activity of overexpressed EZH2 may well be inhibited by Akt-mediated phosphorylation. Regulation of *HOXA* expression is even more complex, involving other histone marks, noncoding RNA, and microRNA-mediated regulation depending on the cellular context (43). Because epigenetic mechanisms are interdependent, PI3K-driven changes in H3K27 methylation may influence additional histone modifications, either directly or indirectly. In fact, the PI3K pathway has been linked to other specific histone modifications, such as H3K9 demethylation (44), acetylation of H3K9 and H3K18 (45), and deacetylation of H3K14 (45). Thus, therapeutic agents targeting components of the PI3K pathway may indirectly affect the histone marks of tumor cells. We hypothesize that particular profiles of histone modifications, in conjunction with the status of the PI3K pathway, may influence therapeutic decisions in the future. Indeed, whereas the histone profile of malignant cells is not currently used to direct therapeutic decisions, histone modifications are strongly correlated with clinical outcome of tumor patients (46–50).

Considerable focus has been placed on developing chemotherapeutic agents to inhibit mTOR, a downstream effector of the PI3K pathway that is an important regulator of cell growth and metabolism (51). Whereas these agents are expected to suppress the growth effects of the mTOR pathway, it is less clear whether mTOR is a factor regulating the expression of *HOXA* genes in GBM. If these domains of transcriptional activation contribute to tumor growth *in vivo*, mTOR inhibitors alone may be suboptimal for improving the outcome in a subset of GBM patients. PI-103, a recently reported agent that dually inhibits PI3K and mTOR in glioma cells (52) or similar agents may prove more efficacious.

MGMT promoter methylation is a favorable prognostic indicator in GBM but is limited in its clinical applicability to individual patients. *HOXA9* expression is a marker of poor prognosis, independent of *MGMT* promoter methylation status, and identifies a subset of the patients who, despite apparently favorable *MGMT* promoter methylation, have poor outcomes. Thus, the combined assessment of *HOXA9* expression and *MGMT* methylation status in GBM may prove to be a promising effective prognostic tool. The grade specificity of *HOXA9* expression according to histology and the association with poor outcome among GBM patients suggest that it may be useful as part of a molecular-based classification of gliomas. The prognostic relevance of *HOXA9* expression in new experimental therapies warrants further investigation.

Disclosure of Potential Conflicts of Interest

No potential conflicts of interest were disclosed.

Acknowledgments

We thank Drs. Corey Largmann and H. Jeffrey Lawrence for helpful discussion regarding *HOXA9* and for sharing retroviral constructs, Dr. Russell Pieper for supplying hTERT/E6/E7 cells, Dr. Amith Panner for assistance with molecular techniques, Dr. Susan Chang for helpful discussion regarding the clinical management of GBM patients, and Drs. Scott Vandenberg and Andrew Bollen for neuropathological assessment of tumors used in this study.

Grant Support

NIH grants NIH CA094971 (J.F. Costello) and NIH/NCI F32 CA113039-01 (J.S. Smith); Karen Osney Brownstein Endowed Chair (J.F. Costello); UC Discovery grant Bio05-10501 (J.F. Costello and H.S. Phillips); Portuguese Science and Technology Foundation SFRH/BD/15258/2004 (B.M. Costa); and Luso-American Development Foundation, Portugal 186/06 (B.M. Costa).

The costs of publication of this article were defrayed in part by the payment of page charges. This article must therefore be hereby marked *advertisement* in accordance with 18 U.S.C. Section 1734 solely to indicate this fact.

Received 6/17/09; revised 11/4/09; accepted 11/5/09; published OnlineFirst 1/12/10.

References

1. Smith JS, Tachibana I, Passe SM, et al. PTEN mutation, EGFR amplification, and outcome in patients with anaplastic astrocytoma and glioblastoma multiforme. J Natl Cancer Inst 2001;93:1246–56.
2. Esteller M, Garcia-Foncillas J, Andion E, et al. Inactivation of the DNA-repair gene MGMT and the clinical response of gliomas to alkylating agents. N Engl J Med 2000;343:1350–4.
3. Hegi ME, Diserens AC, Gorlia T, et al. MGMT gene silencing and benefit from temozolomide in glioblastoma. N Engl J Med 2005;352:997–1003.
4. Mellinghoff IK, Wang MY, Vivanco I, et al. Molecular determinants of the response of glioblastomas to EGFR kinase inhibitors. N Engl J Med 2005;353:2012–24.
5. Costello JF, Futscher BW, Kroes RA, Pieper RO. Methylation-related chromatin structure is associated with exclusion of transcription factors from and suppressed expression of the O-6-methylguanine DNA methyltransferase gene in human glioma cell lines. Mol Cell Biol 1994;14:6515–21.
6. Costello JF, Futscher BW, Tano K, Graunke DM, Pieper RO. Graded methylation in the promoter and body of the O6-methylguanine DNA methyltransferase (MGMT) gene correlates with MGMT expression in human glioma cells. J Biol Chem 1994;269:17228–37.
7. Pearson JC, Lemons D, McGinnis W. Modulating Hox gene functions during animal body patterning. Nat Rev Genet 2005;6:893–904.

Published OnlineFirst January 12, 2010; DOI: 10.1158/0008-5472.CAN-09-2189

8. Satokata I, Benson G, Maas R. Sexually dimorphic sterility phenotypes in Hoxa10-deficient mice. Nature 1995;374:460–3.
9. Takahashi Y, Hamada J, Murakawa K, et al. Expression profiles of 39 HOX genes in normal human adult organs and anaplastic thyroid cancer cell lines by quantitative real-time RT-PCR system. Exp Cell Res 2004;293:144–53.
10. Yamamoto M, Takai D, Yamamoto F, Yamamoto F. Comprehensive expression profiling of highly homologous 39 hox genes in 26 different human adult tissues by the modified systematic multiplex RT-pCR method reveals tissue-specific expression pattern that suggests an important role of chromosomal structure in the regulation of hox gene expression in adult tissues. Gene Expr 2003;11:199–210.
11. Neville SE, Baigent SM, Bicknell AB, Lowry PJ, Gladwell RT. Hox gene expression in adult tissues with particular reference to the adrenal gland. Endocr Res 2002;28:669–73.
12. Morgan R. Hox genes: a continuation of embryonic patterning? Trends Genet 2005;22:67–9.
13. Borrow J, Shearman AM, Stanton VP, Jr., et al. The t(7;11)(p15;p15) translocation in acute myeloid leukaemia fuses the genes for nucleoporin NUP98 and class I homeoprotein HOXA9. Nat Genet 1996;12: 159–67.
14. Golub TR, Slonim DK, Tamayo P, et al. Molecular classification of cancer: class discovery and class prediction by gene expression monitoring. Science 1999;286:531–7.
15. Grier DG, Thompson A, Kwasniewska A, McGonigle GJ, Halliday HL, Lappin TR. The pathophysiology of HOX genes and their role in cancer. J Pathol 2005;205:154–71.
16. Murat A, Migliavacca E, Gorlia T, et al. Stem cell-related "self-renewal" signature and high epidermal growth factor receptor expresison associated with resistance to concomitant chemoradiotherapy in glioblastoma. J Clin Oncol 2008;26:3015–24.
17. Abdel-Fattah R, Xiao A, Bomgardner D, Pease CS, Lopes MB, Hussaini IM. Differential expression of HOX genes in neoplastic and non-neoplastic human astrocytes. J Pathol 2006;209:15–24.
18. Calvo KR, Knoepfler PS, Sykes DB, Pasillas MP, Kamps MP. Meis1a suppresses differentiation by G-CSF and promotes proliferation by SCF: potential mechanisms of cooperativity with Hoxa9 in myeloid leukemia. Proc Natl Acad Sci U S A 2001;98:13120–5.
19. Kleihues P, Louis DN, Scheithauer BW, et al. The WHO classification of tumors of the nervous system. J Neuropathol Exp Neurol 2002;61: 215–25; discussion 26-9.
20. Nigro JM, Misra A, Zhang L, et al. Integrated array-comparative genomic hybridization and expression array profiles identify clinically relevant molecular subtypes of glioblastoma. Cancer Res 2005;65: 1678–86.
21. Phillips HS, Kharbanda S, Chen R, et al. Molecular subclasses of high-grade glioma predict prognosis, delineate a pattern of disease progression, and resemble stages in neurogenesis. Cancer Cell 2006;9:157–73.
22. Pandita A, Aldape KD, Zadeh G, Guha A, James CD. Contrasting *in vivo* and *in vitro* fates of glioblastoma cell subpopulations with amplified EGFR. Genes Chromosomes Cancer 2004;39:29–36.
23. Sarkaria JN, Carlson BL, Schroeder MA, et al. Use of an orthotopic xenograft model for assessing the effect of epidermal growth factor receptor amplification on glioblastoma radiation response. Clin Cancer Res 2006;12:2264–71.
24. Yang L, Clarke MJ, Carlson BL, et al. PTEN loss does not predict for response to RAD001 (Everolimus) in a glioblastoma orthotopic xenograft test panel. Clin Cancer Res 2008;14:3993–4001.
25. Millar DS, Warnecke PM, Melki JR, Clark SJ. Methylation sequencing from limiting DNA: embryonic, fixed, and microdissected cells. Methods 2002;27:108–13.
26. Rhodes DR, Yu J, Shanker K, et al. ONCOMINE: a cancer microarray database and integrated data-mining platform. Neoplasia 2004;6:1–6.
27. Sun L, Hui AM, Su Q, et al. Neuronal and glioma-derived stem cell factor induces angiogenesis within the brain. Cancer Cell 2006;9: 287–300.
28. Cha TL, Zhou BP, Xia W, et al. Akt-mediated phosphorylation of EZH2 suppresses methylation of lysine 27 in histone H3. Science 2005;310:306–10.
29. Rinn JL, Kertesz M, Wang JK, et al. Functional demarcation of active and silent chromatin domains in human HOX loci by noncoding RNAs. Cell 2007;129:1311–23.
30. Steck PA, Pershouse MA, Jasser SA, et al. Identification of a candidate tumour suppressor gene, MMAC1, at chromosome 10q23.3 that is mutated in multiple advanced cancers. Nat Genet 1997;15:356–62.
31. Li J, Yen C, Liaw D, et al. PTEN, a putative protein tyrosine phosphatase gene mutated in human brain, breast, and prostate cancer. Science 1997;275:1943–7.
32. Adachi J, Ohbayashi K, Suzuki T, Sasaki T. Cell cycle arrest and astrocytic differentiation resulting from PTEN expression in glioma cells. J Neurosurg 1999;91:822–30.
33. Lamb J, Crawford ED, Peck D, et al. The connectivity map: using gene-expression signatures to connect small molecules, genes, and disease. Science 2006;313:1929–35.
34. Frigola J, Song J, Stirzaker C, Hinshelwood RA, Peinado MA, Clark SJ. Epigenetic remodeling in colorectal cancer results in coordinate gene suppression across an entire chromosome band. Nat Genet 2006;38:540–9.
35. Novak P, Jensen T, Oshiro MM, et al. Epigenetic inactivation of the HOXA gene cluster in breast cancer. Cancer Res 2006;66:10664–70.
36. Stransky N, Vallot C, Reyal F, et al. Regional copy number-independent deregulation of transcription in cancer. Nat Genet 2006;38: 1386–96.
37. Chakravarti A, Zhai G, Suzuki Y, et al. The prognostic significance of phosphatidylinositol 3-kinase pathway activation in human gliomas. J Clin Oncol 2004;22:1926–33.
38. Kroon E, Thorsteinsdottir U, Mayotte N, Nakamura T, Sauvageau G. NUP98-HOXA9 expression in hemopoietic stem cells induces chronic and acute myeloid leukemias in mice. EMBO J 2001;20:350–61.
39. Schwartz YB, Pirrotta V. Polycomb silencing mechanisms and the management of genomic programmes. Nat Rev Genet 2007;8:9–22.
40. Bracken AP, Pasini D, Capra M, Prosperini E, Colli E, Helin K. EZH2 is downstream of the pRB-E2F pathway, essential for proliferation and amplified in cancer. EMBO J 2003;22:5323–35.
41. Varambally S, Dhanasekaran SM, Zhou M, et al. The polycomb group protein EZH2 is involved in progression of prostate cancer. Nature 2002;419:624–9.
42. Liang Y, Diehn M, Watson N, et al. Gene expression profiling reveals molecularly and clinically distinct subtypes of glioblastoma multiforme. Proc Natl Acad Sci U S A 2005;102:5814–9.
43. Popovic R, Erfurth F, Zeleznik-Le N. Transcriptional complexity of the HOXA9 locus. Blood Cells Mol Dis 2008;40:156–9.
44. Chen YL, Law PY, Loh HH. NGF/PI3K signaling-mediated epigenetic regulation of δ opioid receptor gene expression. Biochem Biophys Res Commun 2008;368:755–60.
45. Sakamoto K, Iwasaki K, Sugiyama H, Tsuji Y. Role of the tumor suppressor PTEN in antioxidant responsive element-mediated transcription and associated histone modifications. Mol Biol Cell 2009;20: 1606–17.
46. Seligson DB, Horvath S, Shi T, et al. Global histone modification patterns predict risk of prostate cancer recurrence. Nature 2005;435: 1262–6.
47. Kahl P, Gullotti L, Heukamp LC, et al. Androgen receptor coactivators lysine-specific histone demethylase 1 and four and a half LIM domain protein 2 predict risk of prostate cancer recurrence. Cancer Res 2006;66:11341–7.
48. Elsheikh SE, Green AR, Rakha EA, et al. Global histone modifications in breast cancer correlate with tumor phenotypes, prognostic factors, and patient outcome. Cancer Res 2009;69:3802–9.
49. Barlesi F, Giaccone G, Gallegos-Ruiz MI, et al. Global histone modifications predict prognosis of resected non small-cell lung cancer. J Clin Oncol 2007;25:4358–64.
50. Seligson DB, Horvath S, McBrian MA, et al. Global levels of histone modifications predict prognosis in different cancers. Am J Pathol 2009;174:1619–28.
51. Reardon DA, Quinn JA, Vredenburgh JJ, et al. Phase 1 trial of gefitinib plus sirolimus in adults with recurrent malignant glioma. Clin Cancer Res 2006;12:860–8.
52. Fan QW, Knight ZA, Goldenberg DD, et al. A dual PI3 kinase/mTOR inhibitor reveals emergent efficacy in glioma. Cancer Cell 2006;9: 341–9.

Published OnlineFirst January 12, 2010; DOI: 10.1158/0008-5472.CAN-09-2189

Cancer Research
The Journal of Cancer Research (1916–1930) | The American Journal of Cancer (1931–1940)

AACR American Association for Cancer Research

Reversing *HOXA9* Oncogene Activation by PI3K Inhibition: Epigenetic Mechanism and Prognostic Significance in Human Glioblastoma

Bruno M. Costa, Justin S. Smith, Ying Chen, et al.

Cancer Res 2010;70:453-462. Published OnlineFirst January 12, 2010.